Materials Science and Engineering A 528 (2011) 1442–1447

Contents lists available at ScienceDirect

Materials Science and Engineering A

journal homepage: www.elsevier.com/locate/msea

Annealing effects on microstructure and coercive field of ferritic–martensitic ODS Eurofer steel

R.A. Renzetti[a], H.R.Z. Sandim[a,*], M.J.R. Sandim[a], A.D. Santos[b], A. Möslang[c], D. Raabe[d]

[a] Escola de Engenharia de Lorena – USP, 12600-970 Lorena, SP, Brazil
[b] Instituto de Física – USP, 05314-970 São Paulo, SP, Brazil
[c] Karlsruher Institut für Technologie (KIT), IMF I, D-72061 Karlsruhe, Germany
[d] Max-Planck Institut für Eisenforschung (MPI-E), D-40237 Düsseldorf, Germany

ARTICLE INFO

Article history:
Received 30 August 2010
Received in revised form 13 October 2010
Accepted 18 October 2010

Keywords:
Steel
Magnetic measurements
Coercive field
Recrystallization
EBSD
ODS

ABSTRACT

Oxide dispersion strengthened reduced-activation ferritic–martensitic steels are promising candidates for applications in future fusion power plants. Samples of a reduced activation ferritic–martensitic 9 wt.%Cr-oxide dispersion strengthened Eurofer steel were cold rolled to 80% reduction in thickness and annealed in vacuum for 1 h from 200 to 1350 °C to evaluate its thermal stability. Vickers microhardness testing and electron backscatter diffraction (EBSD) were used to characterize the microstructure. The microstructural changes were also followed by magnetic measurements, in particular the corresponding variation of the coercive field (H_c), as a function of the annealing treatment. Results show that magnetic measurements were sensitive to detect the changes, in particular the martensitic transformation, in samples annealed above 850 °C (austenitic regime).

1. Introduction

Important microstructural changes occur during annealing of deformed metals including recovery of structural defects, recrystallization, grain growth and other phase transformations. These changes can be followed by several characterization techniques including classical metallography, hardness testing and electron backscatter diffraction. In this work, we investigate the annealing behavior of a ferromagnetic material presenting coercivity below 30 Oe for the initial condition. The magnetic properties of ferritic steels are strongly dependent on their microstructure [1]. In particular, the microstructure affects the motion of magnetic domain walls and, in consequence, the characteristic parameters of the hysteresis loop. High and low angle boundaries, dislocations, precipitates and solute atoms act as pinning sites against magnetic domain wall motion [1–6]. Among several magnetic parameters the coercive field (H_c), which is the intensity of the magnetic field needed to reduce the magnetization of a ferromagnetic material to zero after it has reached magnetic saturation, can be used to monitor microstructural changes in different materials [2,3,7]. The coercive field H_c reflects the amount and strength of pinning of domain walls and is strongly dependent on microstructural parameters such as grain size (d) and dislocation density (ρ). Theoretical considerations demonstrate that H_c is proportional to the square root of ρ, $H_c \propto \sqrt{\rho}$, and directly proportional to the inverse of d, $H_c \propto 1/d$ [1–3].

The thermal stability of reduced-activation 9%Cr oxide dispersion strengthened (ODS) ferritic/martensitic (RAFM) steel in the ferritic regime was reported elsewhere [8]. The RAFM steels have been widely investigated due to their high irradiation resistance, high mechanical strength, reasonable ductility (about 15–20%) and low activation. The chemical composition of an ODS RAFM steel should make radioactive activation, when exposed to neutron irradiation, as low and quickly decaying as possible to allow re-use or disposal. Due to these properties, these materials are good candidates for high temperature applications for nuclear fusion technology [9–11]. Typically, the RAFM steels are limited to an upper operating temperature of about 550 °C. However, the replacement of RAFM steel by suitable oxide dispersion strengthened (ODS) alloy increases the operating temperature to about 650 °C or even more [10,12]. Only a few works reported about magnetic properties of RAFM steels developed for the requirements of the European fusion technology program [13,14]. In previous works [13,14] only non-ODS steels like Eurofer 97 in the as-tempered condition were investigated. In the present work, therefore, we report about the annealing effects on the microstructure and coercive field of an ODS RAFM steel. The analysis is extended for samples

* Corresponding author at: Escola de Engenharia de Lorena – USP, P. O. Box 116, 12600-970 Lorena, SP, Brazil. Tel.: +55 12 3159 9916; fax: +55 12 3153 3006.
E-mail address: hsandim@demar.eel.usp.br (H.R.Z. Sandim).

0921-5093/$ – see front matter © 2010 Elsevier B.V. All rights reserved.
doi:10.1016/j.msea.2010.10.051

annealed at much higher temperatures in the austenite phase followed by air cooling where martensite forms. The specimens were characterized by conventional metallography, electron backscatter diffraction (EBSD), Vickers hardness measurements and magnetic measurements.

2. Experimental

The ODS-Eurofer steel was processed by a powder metallurgy route including mechanical alloying of powders, hot isostatic pressing and further hot rolling followed by tempering. Details are given elsewhere [15]. The nominal composition of ODS-Eurofer used in the present investigation was 9Cr–1W–0.08Ta–0.2V–0.07C–0.4Mn–0.3Y_2O_3 (wt.%). The tempered steel was cold rolled to 80% thickness reduction in multiple passes. Samples were annealed in vacuum from 200 °C up to 1350 °C for 1 h followed by air cooling. Only the specimens annealed in the austenitic regime (900–1350 °C) were tempered at 550 °C and 750 °C for 2 h in vacuum in sealed glass.

Vickers microhardness testing was performed using a load of 200 g for 30 s on the longitudinal sections of polished samples. A JEOL-6500F field emission gun scanning electron microscope (FEG-SEM) operating at 15 kV was used to image the microstructure of the specimens annealed at 800, 1100 and 1350 °C for 1 h. High resolution microtexture evaluation with a step size of 50 nm was conducted by automated acquisition and further indexing of Kikuchi patterns after image processing in a TSL system interfaced to the scanning electron microscope [16,17].

The magnetic measurements were performed using a vibrating sample magnetometer (VSM) from EG&G Princeton Applied Research. The maximum applied field was 16 kOe. The hysteresis loops were carried out at room temperature using the following sweep rates: 0.4 kOe/min for $|H| < 0.5$ kOe, 1.8 kOe/min for $0.5 < |H| < 5$ kOe and 10 kOe/min for $6 < |H| < 16$ kOe. Using this protocol we obtained complete magnetization curves in a suitable time (25 min each) and determined the coercive field with an accuracy of ±5 Oe.

The methodology for the determination of the coercive field from the hysteresis loop is discussed in Section 3. Taking into account the possibility of anisotropic effects, two sets of samples were cut into approximate dimensions 5 mm × 3 mm × 1.5 mm, with the larger dimension taken at two conditions, viz. parallel and perpendicular to the rolling direction (RD). The magnetization curves were obtained with the external field parallel to the larger dimension of the sample (5 mm). The hysteresis loops were obtained for two field configurations, i.e. the magnetic field is applied parallel and perpendicular to RD. The hysteresis loops were not corrected for demagnetization effects as it has no significant effect on the coercive field values [14].

3. Results and discussion

3.1. Microstructure

The microstructure of 9%Cr-ODS-RAFM Eurofer steel in the as-received condition consists of grains with size of about 3 μm [5]. Both nanoscale Y_2O_3 and coarse $M_{23}C_6$ (M = Cr, Fe) particles are found dispersed in the ferritic Fe–Cr matrix with volume fractions of about 0.5% and 1.5%, respectively [8,18,19].

The critical temperatures A_{c1}, A_{c3} and M_s determined by dilatometry were reported to be 850 °C, 940 °C and 350 °C, respectively, for a heating rate of 5 °C/s [8]. The softening curve of 9%Cr-ODS Eurofer steel annealed within the ferritic phase field, i.e., below 850 °C, shows a drop in hardness of about 7%, as shown in Fig. 1. This small amount of softening is caused by

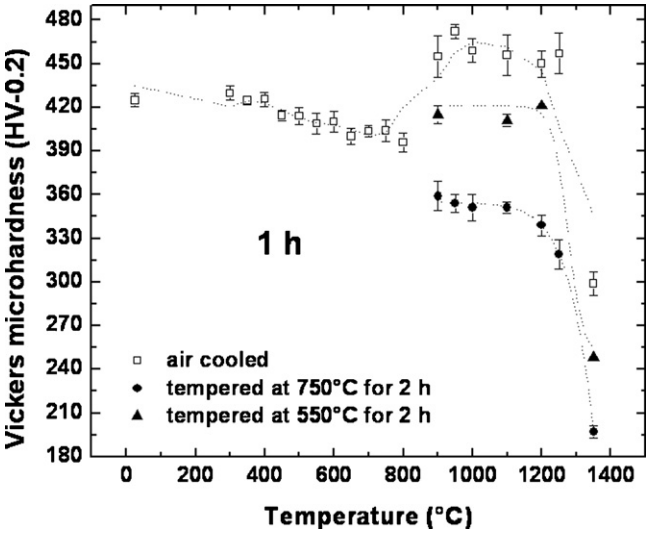

Fig. 1. Softening behavior of 80% cold-rolled 9%Cr-ODS-RAFM Eurofer steel followed by 1 h annealing at several temperatures (open symbols). Results for tempered conditions are also shown (full symbols).

static recovery[1] as the volume fraction of recrystallized grains after annealing at 800 °C for 1 h is below 0.1. Such a behavior is attributed to the presence of nanosized Y_2O_3 particles which prevent the rearrangement of dislocations and the migration of high angle boundaries during annealing [8]. Contrasting to the effect promoted by large carbide particles ($M_{23}C_6$) which stimulate static recrystallization, the influence of nanosized oxide particles is much more pronounced, rendering recrystallization very sluggish. It is worth mentioning that the presence of large non-deformable particles contributes to an increase in the dislocation density around particles (deformation zones). With increasing strain, large lattice rotations develop and mobile deformation-induced boundaries may trigger recrystallization. Details of the microstructural characterization of 9%Cr-ODS-Eurofer steel in the ferritic phase field are given elsewhere [8].

Important changes in the microstructure occur when annealing is performed at higher temperatures. Above 850 °C, a martensitic structure appears even upon air cooling. The martensitic transformation is accompanied by significant hardening due to the increase in dislocation density and by the increase in interfaces density associated with the phase transformation. Fig. 1 reveals that the hardness remains almost unchanged when annealing is performed between 900 °C and 1250 °C leveling at about 450 HV and it drops substantially to about 300 HV after annealing at 1350 °C. The effect of 2 h-tempering either at 550 °C or at 750 °C on the softening behavior is also shown in Fig. 1. Softening occurs due to intensive dislocation annihilation, carbide precipitation and later grain- and particle coarsening during tempering. The tempered microstructure consists of ferritic grains and carbides, mainly $M_{23}C_6$ and MC types [15,20,21]. Notice that tempering at 750 °C is much more effective than at 550 °C to soften this steel. One possible explanation for the much lower value of hardness found for the sample annealed at 1350 °C for 1 h compared to the samples annealed between 900 °C and 1100 °C is the occurrence of intense austenite grain growth.

[1] In static recovery, there occurs dislocation annihilation and/or rearrangement followed by rapid subgrain growth. The term "*static*" refers to the changes occurring during annealing of deformed metals whereas "*dynamic*" refers to similar microstructural changes which occur during straining.

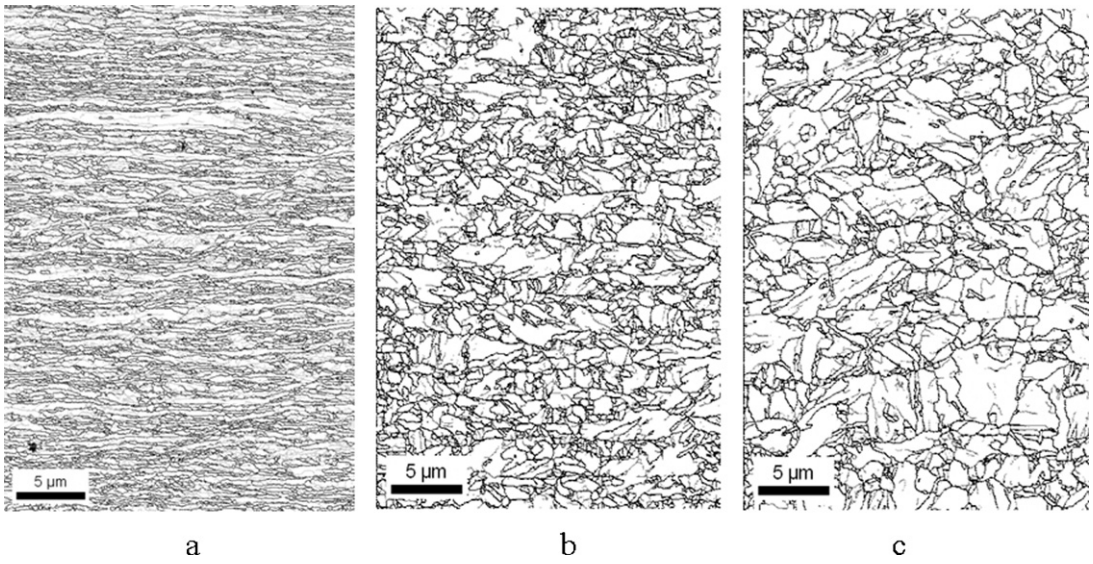

Fig. 2. High resolution EBSD scans in longitudinal sections of 80% cold-rolled 9%Cr-ODS-RAFM Eurofer steel annealed for 1 h at: (a) 800 °C for 1 h; (b) 1100 °C for 1 h; (c) 1350 °C. High angle boundaries (above 15° misorientation) are marked by black lines. Low angle boundaries are marked by gray lines. RD is parallel to the scale bar.

The EBSD technique was used to image the microstructure at the grain and sub-grain scale. The advantage of using EBSD is that it allows the observation of grain boundaries in the microstructure much more clearly than by using conventional metallographic inspection (light optical or scanning electron microscopy). Important differences in grain size and morphology are noticeable. The microstructure of the 9%Cr-ODS Eurofer steel annealed at 800 °C for 1 h consists of elongated grains aligned parallel to the rolling direction, as shown in Fig. 2a. The mean grain size of the recovered structure cannot be easily determined since grains are non-equiaxed. Fig. 2b and c shows the corresponding microstructures after annealing for 1 h in the austenitic phase field (1100 °C and 1350 °C, respectively) followed by air cooling. The resulting microstructures are very different. Both display a martensite structure and differ mainly in terms of grain size, Fig. 3. Their average grain sizes are 1.2 μm and 1.7 μm, respectively. Annealing at 1350 °C promotes intense coarsening and grains with sizes above 5 μm appear. The size distribution for the sample annealed to 1350 °C is also slightly broader than at 1100 °C.

The microtextures of samples annealed at 800, 1100 and 1350 °C were determined by EBSD, as shown in Fig. 4. Only sections of $\varphi_2 = 0°$ and 45° of the orientation distribution function (ODF) are shown as they contain the most relevant texture components of Fe–Cr steels [22]. The textures of bcc steels can be described by a set of texture fibers such as the α-fiber collecting all grains with a ⟨1 1 0⟩ direction parallel to the rolling direction (RD) and the γ-fiber summarizing all crystals with a {1 1 1} plane parallel to the sheet surface [23–25]. Results for the sample annealed at 800 °C for 1 h shows texture components belonging to α and γ fibers commonly found in cold rolled bcc steels. It is worth mentioning that static recovery is the main softening mechanism acting below 850 °C (ferritic phase field). The α fiber has a maximum close to {1 1 3}⟨1 1 0⟩ whereas the γ fiber is incomplete with a maximum centered in {1 1 1}⟨1 1 0⟩. The rotated cube component {1 0 0}⟨1 1 0⟩ is also present. The orientation density of the texture is about 7.8 times random. Fig. 4b and c shows the ODF sections for the sample annealed at 1100 °C and 1350 °C. The martensitic transformation changed the texture rendering the γ fiber component a bit sharper [26]. The spread around the ideal orientation of the rotated cube component becomes larger as well. In both conditions the texture intensities are rather weak, being equal to 3.6 and 3.4 times random, respectively.

These changes in the microstructure determined by using classical metallography and Vickers hardness measurements could be also followed by means of magnetic measurements of heat-treated specimens as discussed in the following.

3.2. Magnetic properties

A typical hysteresis loop obtained for the 9%Cr-ODS-RAFM Eurofer steel is displayed in the main panel of Fig. 5. Each sample used for magnetic characterization had a volume of about 23 mm^3. Based on metallographic observations and assuming spherical grains with

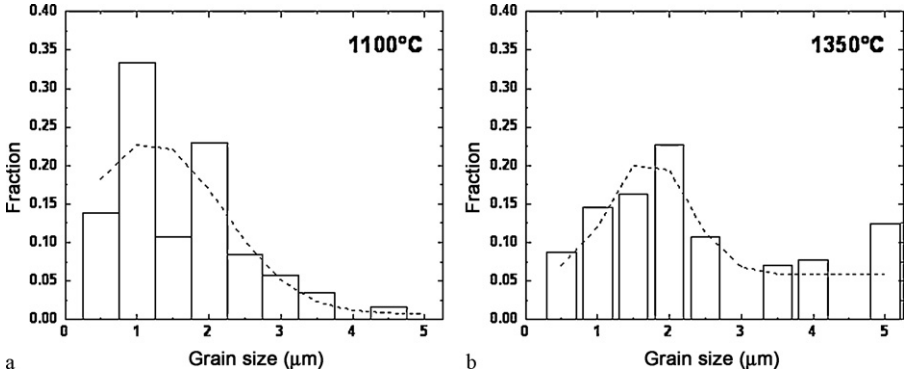

Fig. 3. Grain size distribution of 9%Cr-ODS-RAFM Eurofer steel after 80% cold rolling and 1-h annealing at: (a) 1100 °C; (b) 1350 °C.

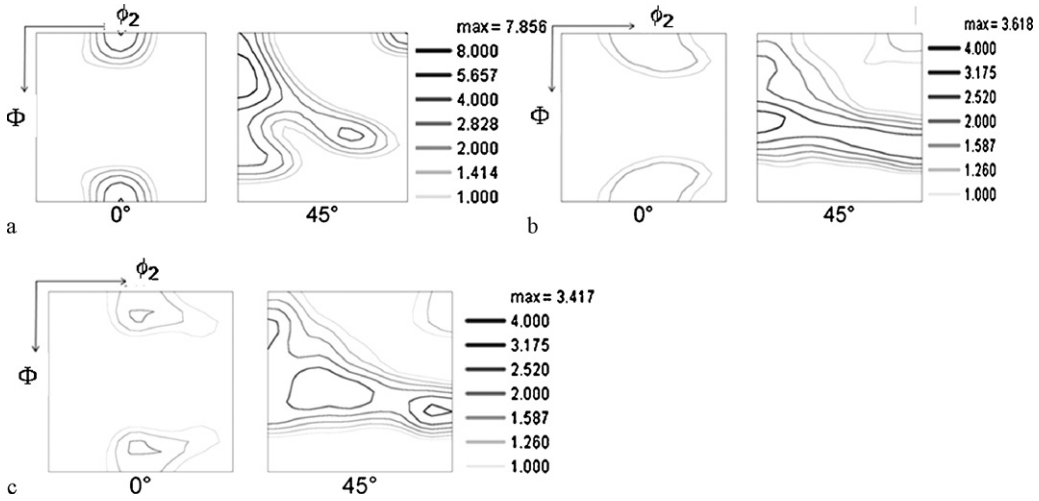

Fig. 4. Orientation distribution function (sections of $\varphi_2 = 0^\circ$ and 45°) of 80% cold-rolled 9%Cr-ODS-RAFM Eurofer steel after 1-h annealing at: (a) 800 °C, (b) 1100 °C and (c) 1350 °C. Euler axes range from 0° to 90°.

sizes of 3–5 μm, the magnetization curves mirror the collective behavior of about 10^8 grains. It is worth mentioning that the grain size slightly varies from one condition to another. Nevertheless the total number of sampled grains is high enough to ensure sufficient statistics of the magnetic measurements. The inset of Fig. 5 shows the central region of the hysteresis loop, where the coercive field values from both branches are indicated.

In this work the coercive field value (H_c) is defined as the average of the absolute values from both branches, in order to eliminate the offset error of the Hall sensor. The H_c values for the 9%Cr-ODS-RAFM Eurofer steel, in both as-rolled (deformed state) and annealed conditions, taken with magnetic field applied parallel to the rolling direction, are displayed in Fig. 6. In the same figure, the corresponding Vickers microhardness values (HV) are shown for comparison.

Fig. 6 shows that H_c and hardness display quite similar trends. However, H_c seems to be more sensitive to the microstructural changes experienced by the 9%Cr-ODS-RAFM Eurofer steel when annealing is performed above 800 °C. As discussed before, for annealing temperatures up to 800 °C, the material undergoes monotonic softening. H_c, in turn, displays a small decrease up to 300 °C, followed by a significant decrease up to 600 °C (about 65%) and then increases slowly until 800 °C. This result is important as there is no change in grain size when annealing is performed up to 800 °C. There are also no significant changes in size of nanosized Y_2O_3 and coarse $M_{23}C_6$ particles [8]. Only static recovery reactions take place within this interval of temperature. Such a decrease rate of H_c between 300 and 600 °C indicates changes in the microstructure due to static recovery that are not detected by microhardness testing. Martínez-de-Guerenu et al. have reported similar observations during annealing of low-carbon steels [2].

In Fig. 6 we observed that the annealing of the 9%Cr-ODS-RAFM Eurofer steel at 900 °C promotes a noticeable increase in the H_c value, about five times higher than the corresponding value at 800 °C. For this temperature range also an increase in hardness was observed, although not of the same proportion, which was correlated with a martensitic transformation. Both, H_c and hardness remain almost unchanged until 1200 °C, followed by a sharp drop at 1350 °C. Such a behavior can be attributed to austenite grain coarsening when the steel is annealed at 1350 °C, Fig. 2. When annealing is performed at such a high temperature the dispersion of the nanosized Y_2O_3 particles becomes less effective to retard grain boundary

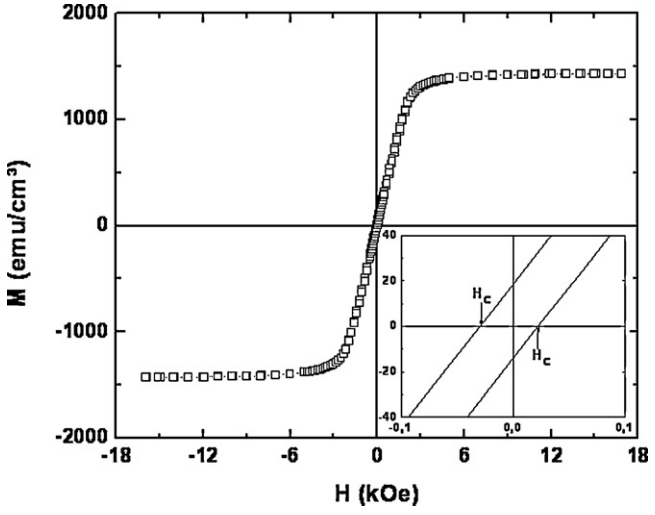

Fig. 5. Hysteresis loop obtained for the 9%Cr-ODS-RAFM Eurofer steel in the as-rolled condition, with field applied parallel to the rolling direction. The inset shows the center of the hysteresis loop, where the coercive field values for both branches are indicated.

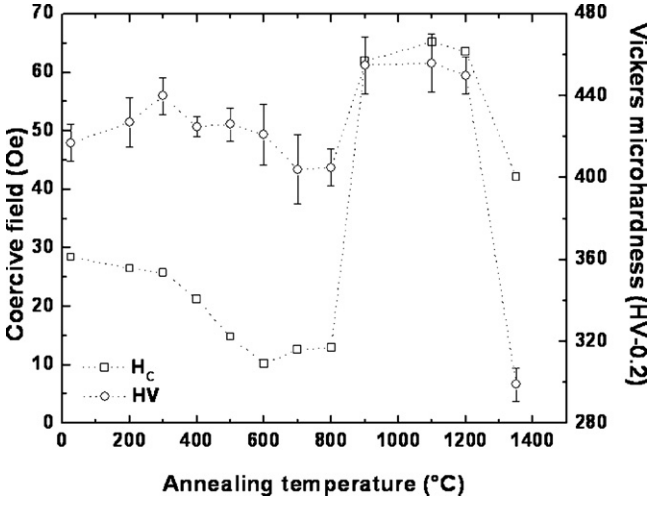

Fig. 6. H_c values obtained for the 9%Cr-ODS-RAFM Eurofer steel for as-rolled and annealed conditions, obtained from the hysteresis loops carried out with field applied parallel to the rolling direction. In the same figure the values of Vickers microhardness for the same annealing conditions are shown.

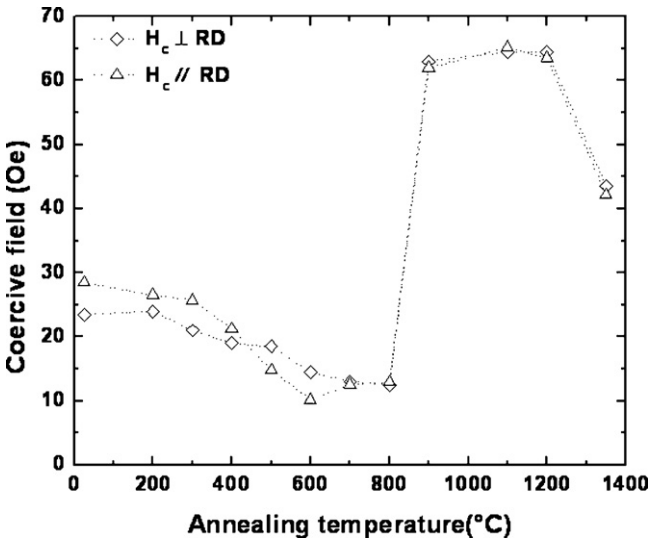

Fig. 7. H_c values obtained for the 9%Cr-ODS-RAFM Eurofer steel for both field configurations: applied parallel and perpendicular to the rolling direction.

migration and hence grain growth. However, it must be noted that the drop at 1350 °C was more intense for hardness than for H_c.

In order to evaluate the influence of anisotropy on the coercive field, Fig. 7 displays the H_c values obtained for a magnetic field applied parallel (as in Fig. 6) and perpendicular to the RD. From this figure no significant differences were found for both field configurations especially for the samples annealed in the austenitic regime where the crystallographic texture is rather weak. As the magnetization is a property with rather pronounced crystallographic anisotropy this means that orientation changes between sample and external field are not expected to occur in the case of weak or random textures.

The results of H_c and hardness for 9%Cr-ODS-RAFM Eurofer steel annealed in the austenitic range followed by tempering are displayed in Fig. 8. In this figure, the H_c values were obtained for a field applied parallel to RD, as the data displayed in Fig. 5. Annealing within the austenitic field promotes the dissolution of the $M_{23}C_6$ particles and causes a significant increase in the dislocation density due to the martensitic transformation during air cooling, as indicated by the Vickers hardness values. After tempering at the two chosen temperatures, the resulting microstructure consists of a ferritic matrix, nanosized Y_2O_3 particles and coarse $M_{23}C_6$ carbides.

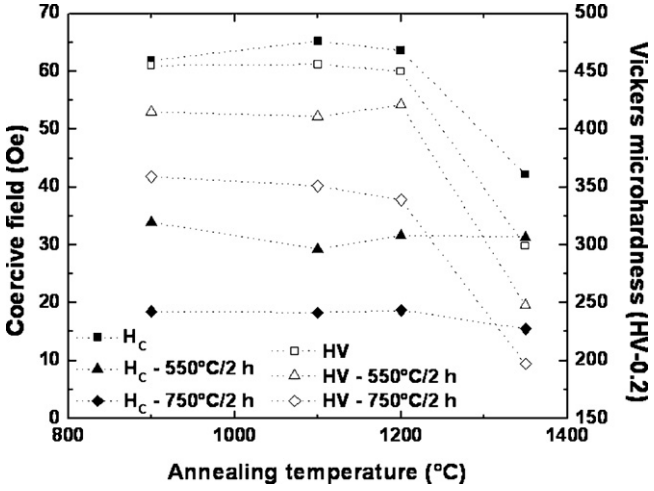

Fig. 8. H_c and HV values obtained for the 9%Cr-ODS-RAFM Eurofer steel annealed in the austenitic field and also tempered at 550 °C and 750 °C for 2 h.

Fig. 8 also reveals that under such conditions the softening is more pronounced for the samples tempered at 750 °C. It must be noticed that the softening behavior of the tempered samples follows the same trend as observed for the samples annealed in the austenitic field (untempered condition).

Regarding the magnetic behavior, the coercive field of the samples annealed in the austenitic phase field shows a pronounced drop when annealing is performed at 1350 °C for 1 h. This behavior is mainly attributed to the increase in grain size in the martensitic structure, as shown in Fig. 2. Concerning the magnetic behavior of the tempered samples we have observed a systematic decrease in the H_c values in comparison with the as-annealed samples. This drop in the H_c values is much more pronounced when tempering is carried out at 750 °C. However, it is also worth mentioning that for the tempered samples the values of H_c remain almost unchanged for all annealing temperatures. During tempering, the main microstructural changes are the intensive dislocation annihilation and concurrent precipitation of Cr-containing carbides. Tempering at these temperatures does not cause any increase in grain size. Therefore, in such a condition, the magnetic behavior of the samples annealed at 1350 °C is likely much more influenced by the presence of $M_{23}C_6$ particles which pin the domain walls than by grain size effects.

4. Summary and conclusions

The microstructure evolution of 9%Cr-ODS-RAFM Eurofer steel during isothermal annealing from 200 °C up to 1350 °C was investigated. In addition to the softening curves, microstructural changes were also followed by magnetic coercive field measurements. Based on the obtained results, the following conclusions can be drawn:

(1) The changes in coercive field and Vickers microhardness display similar trends, i.e. the magnetic properties mirror the microstructure changes upon isothermal annealing within a wide range of temperatures (200–1350 °C).
(2) For samples annealed in the ferritic regime (up to 850 °C) the main softening mechanism is static recovery. However, the relative decrease of H_c was more pronounced than the observed for Vickers microhardness. Such a feature suggests that the magnetic coercive field shows a higher sensitivity to detect microstructural changes related to recovery (dislocation annihilation and subgrain growth).
(3) Both values of H_c and hardness increased for samples annealed in the austenitic regime (above 850 °C) due to the martensitic transformation upon air cooling, but not in the same proportion. Due to intensive austenite grain growth above 1250 °C, we have observed a decrease for both H_c and hardness values.
(4) Tempering promoted the decrease of the absolute values of both H_c and Vickers hardness. Concerning the magnetic behavior of the tempered samples we have observed a systematic decrease in the H_c values in comparison with the as-annealed samples. This drop in the H_c values is much more pronounced when tempering is carried out at 750 °C. The values of H_c in the tempered condition remain nearly unchanged for all annealing conditions. The magnetic behavior of the samples annealed at 1350 °C is likely much more influenced by the presence of $M_{23}C_6$ particles which pin the domain walls than by grain size effects.

Acknowledgments

Authors are grateful to FAPESP (Grants 07/56436-0 and 08/54064-1) and to CNPq (Grant 384.455/2007-4) for the financial

support. Authors are also acknowledged to Dr. Rainer Lindau (KIT, Karlsruhe) for supplying the samples for this investigation and to Mrs. Katja Angenendt (MPI-E, Düsseldorf) for her kind assistance in the EBSD measurements.

References

[1] M.J. Sablik, J. Appl. Phys. 89 (2001) 7254–7256.
[2] A. Martínez-de-Guerenu, F. Arizti, M. Dias-Fuentes, I. Gutiérrez, Acta Mater. 52 (2004) 3657–3664.
[3] M. Oyarzábal, K. Gurruchaga, A. Martínez-de-Guerenu, I. Gutiérrez, ISIJ Int. 47 (2007) 1458–1464.
[4] B.D. Cullity, Introduction to Magnetic Materials, Addison-Wesley, Boston, MA, 1972.
[5] Y.B. Cai, S.K. Chang, ISIJ Int. 47 (2007) 1680–1686.
[6] M.F. de Campos, T. Yonamine, M. Fukuhara, F.J.G. Landgraf, C.A. Achete, F.P. Missell, IEEE Trans. Magn. 42 (2006) 2812–2814.
[7] Y. Sidor, F. Kovac, T. Kvackaj, Acta Mater. 55 (2007) 1711–1722.
[8] H.R.Z. Sandim, R.A. Renzetti, A.F. Padilha, D. Raabe, M. Klimenkov, R. Lindau, A. Möslang, Mater. Sci. Eng. A 527 (2010) 3602–3608.
[9] K. Ehrlich, Fusion Eng. Des. 56–57 (2001) 71–82.
[10] R. Lindau, A. Möslang, M. Rieth, M. Klimenkou, E. Materna-Morris, A. Alamo, A.-A.F. Tavassoli, C. Caryon, A.-M. Lancha, P. Fernandez, N. Baluc, R. Schäublin, E. Diegele, G. Filacchioni, J.W. Resman, B.v.d. Schaaf, E. Lucon, W. Dietz, Fusion Eng. Des. 75–79 (2005) 989–996.
[11] A. Möslang, E. Diegele, M. Klimenkou, R. Lässer, R. Lindau, E. Lucon, E. Materna-Morris, C. Petersen, R. Pippan, J.W. Renaman, M. Rieth, Nucl. Fusion 45 (2005) 649–655.
[12] A. Möslang, Ch. Adelhelm, R. Heidinger, Int. J. Mater. Res. 99 (2008) 1045–1054.
[13] A.A.F. Tavassoli, et al., J. Nucl. Mater. 329–333 (2004) 257–262.
[14] K. Mergia, N. Boukos, J. Nucl. Mater. 373 (2008) 1–8.
[15] M. Klimiankou, R. Lindau, A. Moslang, J. Nucl. Mater. 367–370 (2007) 173.
[16] R. Song, D. Ponge, R. Kaspar, D. Raabe, Z. Metallk. 95 (2004) 513–517.
[17] R. Song, D. Ponge, D. Raabe, R. Kaspar, Acta Mater. 53 (2004) 845–858.
[18] R. Schaeublin, T. Leguey, P. Spätig, N. Baluc, M. Victoria, J. Nucl. Mater. 307–311 (2002) 778–782.
[19] M. Klimiankou, R. Lindau, A. Möslang, J. Nucl. Mater. 329–333 (2004) 347–351.
[20] K. Maruyama, K. Sawada, J. Koike, ISIJ Int. 41 (2001) 641–653.
[21] H. Sakasegawa, T. Hirose, A. Kohyama, Y. Katoh, T. Harada, K. Asakura, T. Kumagai, J. Nucl. Mater. 307–311 (2002) 490–494.
[22] D. Raabe, K. Lücke, Mater. Sci. Technol. 9 (1993) 302–312.
[23] M. Hölscher, D. Raabe, K. Lücke, Steel Res. 62 (1991) 567–575.
[24] D. Raabe, K. Lücke, Scripta Metall. Mater. 27 (1992) 1533–1538.
[25] B. Hutchinson, Philos. Trans. R. Soc. Lond. A 357 (1999) 1471–1485.
[26] D. Raabe, M. Ylitalo, Metal. Mater. Trans. A 27 (1996) 49–57.